Journal of Non-Crystalline Solids 278 (2000) 24–34

# Method to estimate crystal/liquid surface energy by dissolution of subcritical nuclei

Vladimir M. Fokin [a,1], Edgar D. Zanotto [a,*], Juern W.P. Schmelzer [b]

[a] *LaMaV – Vitreous Materials Laboratory, Department of Materials Engineering, Federal University of São Carlos, 13565-905 São Carlos, SP, Brazil*

[b] *Department of Physics, University of Rostock, 18051 Rostock, Germany*

Received 5 July 2000

**Abstract**

Within the framework of the classical nucleation theory (CNT) the nucleus–liquid surface energy ($\sigma$) is one of the most important parameters to predict or analyze nucleation kinetics in undercooled liquids. However, the few methods proposed to determine $\sigma$ are based on the direct use of nucleation rate data and, thus, do not allow an independent test of the theory. In the present paper, this parameter is estimated without direct use of nucleation rate data. Instead, we provide further experimental evidence for the dissolution of sub-critical nuclei at several development temperatures and use this effect to estimate the nucleus–liquid surface energy. The results of the present analysis demonstrate that, in agreement with a new approach for the description of nucleation processes, not only the surface energy but also the driving force for nucleation have quite different values from those of the evolving macrophases. The possible implications of this result for the understanding of crystal nucleation in liquids are discussed. 

## 1. Introduction

About a hundred years ago, Gustav Tammann [1] analyzed crystallization processes in undercooled organic liquids at low temperatures in the vicinity of the glass transition temperature, $T_g$. In these analyses, he applied a procedure to experimentally observe and determine the number density of crystal nuclei. Since the typical sizes of critical nuclei in liquids are undetectable by experimental techniques, they have first to be developed to visible sizes. The procedure proposed by Tammann is now known as the Tammann or 'development' method and is frequently used by materials scientists in the determination of nucleation kinetics. The method consists in developing the crystals nucleated at a low temperature, $T_n$, at a higher temperature, $T_d > T_n$, up to a size visible under an optical or electron microscope. The development temperature, $T_d$, should be chosen so that the following conditions are met for the nucleation rate and crystal growth velocity, $I$ and $U$, respectively: $I(T_n) \gg I(T_d)$ and $U(T_d) \gg U(T_n)$.

After a lapse of seventy years, Ito et al. [2] and Filipovich and Kalinina [3] independently applied

* Corresponding author. Tel.: +55-162 74 8250; fax: +55-162 61 5404.

*E-mail address:* dedz@power.ufscar.br (E.D. Zanotto).

[1] On sabbatical leave from the Institute of Silicate Chemistry, Odoevskogo 24/2, 199155 St. Petersburg, Russia.

0022-3093/00/$ - see front matter 
PII: S0022-3093(00)00335-5

Tammann's method to study the crystal nucleation kinetics of lithium dissilicate glasses. Since then, this method has been widely employed for glass crystallization studies. In using Tammann's method, one usually assumes that the 'development' process includes only the growth of pre-existing crystals that were nucleated at a lower temperature. However, according to the classical nucleation theory (CNT), the size of a critical nucleus, $r^*$, increases with temperature due to the decrease in the thermodynamic driving force (e.g., [4]) and hence $r^*(T_d) > r^*(T_n)$. Thus, only those crystals that have reached a size $r^*(T_d)$ during heat-treatment at $T_n$ (due to crystal growth at $T_n$) are able to grow at the development temperature, $T_d$, while those crystals having sizes smaller than $r^*(T_d)$ dissolve at $T_d$. Volmer and Weber [5] have emphasized this point on commenting Tammann's results in 1926.

The number of dissolving crystals increases when the difference between $T_n$ and $T_d$ and, thus between $r^*(T_n)$ and $r^*(T_d)$ increases. Hence the number of developed crystals *decreases* with increasing $T_d$. Indeed, a reduction in the number of developed crystals with increasing $T_d$ has been found experimentally for organic liquids [6] as well as for silicate glasses [7]. In the present paper, we employ this effect for a determination of the nucleus–liquid interfacial free energy.

The nucleus–liquid interfacial free energy, $\sigma$, is one is the most important parameters of CNT controlling the nucleation rate $(I = (A/\eta) \exp(-A'\sigma^3/T\Delta G^2)$, where $A$ and $A'$ are constants, $\eta$ is the viscosity coefficient and $\Delta G$ is the thermodynamic driving force). In accordance with Gibbs' classical approach for the description of heterogeneous systems [8], $\Delta G$ is usually determined as the difference in the Gibbs free energies per mole or particle in the respective *macroscopic* crystalline and liquid phases. Thus, to predict or analyze nucleation kinetics in undercooled liquids with CNT one needs to know the value of the interfacial free energy. To this date, however, reliable, direct, experimental methods to determine the crystal nucleus–liquid surface energy are not known [9].

To estimate the crystal–liquid surface energy the (semi-empirical) Scapski–Turnbull equation [10] is often used

$$\sigma_T = \alpha \Delta H_m V_m^{-2/3} N_A^{-1/3}, \quad (1)$$

where $\Delta H_m$ is the molar heat of melting, $V_m$ is the molar volume, $N_A$ is Avogadro's number and $\alpha$ is an empirical coefficient obtained from nucleation experiments. In particular, when the capillarity approximation of CNT is used ($\sigma =$ constant), $\alpha$ varies from about 0.40–0.55 for silicate glasses [11]. Eq. (1) was derived on the assumption that the surface energy per structural unit, located at the crystal-melt interface, is proportional to the melting enthalpy per structural unit.

The few existing methods for *experimental* determination of $\sigma$ are quite complex and are generally based on nucleation experiments, involving certain additional assumptions. For instance, the assumption that $\sigma$ does not depend on temperature allows the estimation of $\sigma$ from a fit of nucleation rate data at different temperatures to CNT. However, this approach leads to drastic discrepancies between the magnitudes of calculated and experimentally observed nucleation rates [12,13].

An alternative procedure is the calculation of $\sigma$ from CNT using the *theoretical* pre-exponential term of the nucleation rate equation and experimental nucleation rate data. In doing so, the time lag in nucleation [14] or the viscosity coefficient [15] is used to estimate the kinetic barrier for nucleation. In the latter case, the Stokes–Einstein equation is employed to correlate the kinetic barrier with the glass viscosity. In both cases the calculations lead to a temperature-dependent surface energy with a positive coefficient, i.e. to an increase of $\sigma$ with temperature. This effective increase of $\sigma$ has been widely discussed [16,17]. However, it has been demonstrated [17] that the apparent temperature dependence of $\sigma$ can be attributed to the size dependence of the specific surface energy expressed, for example, by Tolman's equation.

A new method for the determination of the crystal–liquid surface energy was recently proposed and applied to lithium disilicate glasses [18]. That method is based upon the use of nucleation data in conjunction with an expression for transient nucleation. To calculate $\sigma$ by this method it is necessary that both the nucleation rate and induction periods be obtained from single-stage

nucleation experiments. The results of [18] also indicate an apparent positive temperature coefficient for $\sigma$.

As it becomes evident from the above summary, the previous attempts to determine the crystal–liquid surface energy rely on several assumptions and have an additional disadvantage; once $\sigma$ is determined from nucleation experiments, the theory looses its predictive power. Thus, the development of new methods to determine $\sigma$ is highly desirable. The independent determination of $\sigma$ is an open issue and every contribution to its solution is of general interest.

In the present paper, we give further experimental evidence for the dissolution of sub-critical nuclei at several development temperatures and use this effect to estimate the nucleus–liquid surface energy. First we present the theoretical background of the method employed to estimate the surface energy. Then, we describe the experiments performed and give new evidence for the dissolution of sub-critical nuclei in two silicate glasses. Next, the experimental results are used for an estimation of $\sigma$. Finally, we discuss the results of surface-energy obtained and compare them with those estimated by other methods. This comparison leads to important consequences concerning the bulk and surface properties of the critical clusters. A summary completes the paper.

## 2. Theoretical background

The total number of supercritical crystals $N$, nucleated at a temperature $T_n$ in time $t$ is given by

$$N(T_n, r^*(T_n), t) = \int_0^t I(T_n, t')\,dt', \tag{2}$$

where $I$ is nucleation rate and $r^*(T_n)$ the critical radius at the temperature $T_n$.

The number of crystals nucleated in the same thermodynamic conditions, but having a size, $r$, larger than the critical size at the development temperature, $r^*(T_d)$, is

$$N(T_n, r^*(T_d), t) = \int_0^{t-t_0} I(T_n, t')\,dt', \tag{3}$$

$$t_0(T_n, T_d) = \int_{r^*(T_n)}^{r^*(T_d)} \frac{dr}{U(T_n, r)},$$

where $U$ is the crystal growth velocity. Here we take into account the fact that critical clusters with a size $r^*(T_n)$ have to grow at least for a time $t_0$ to reach the size $r^*(T_d)$.

Eqs. (2) and (3) yield

$$N(T_n, r^*(T_n), t) = N(T_n, r^*(T_d), t + t_0). \tag{4}$$

Hence, a $N(T_n, r^*(T_n), t)$ plot agrees with a $N(T_n, r^*(T_d), t)$ plot, with the only difference that the latter is shifted along the time-axis by a time $t_0$. Thus, the development method provides the *correct* value of the steady-state nucleation rate and an *overestimated* (by $t_0$) value of the induction time for nucleation. Then, the kinetic curves, $N(T_n, t)$, obtained with different development temperatures, $T_{d1}$ and $T_{d2} > T_{d1}$, should be shifted from each other by a time $\Delta t_0 = t_{02} - t_{01}$.

The following equation was derived in [7] to estimate this shift:

$$\begin{aligned}\Delta t_0 &= \int_{r^*(T_{d1})}^{r^*(T_{d2})} \frac{dr}{U(T_n, r)} \\ &= \frac{1}{U(T_n, \infty)}\left[r^*(T_{d2}) - r^*(T_{d1}) + r^*(T_n)\ln\frac{r^*(T_{d2}) - r^*(T_n)}{r^*(T_{d1}) - r^*(T_n)}\right].\end{aligned} \tag{5}$$

In the derivation of Eq. (5), a size dependent crystal growth velocity [19] was used

$$U(T, r) = U(T, \infty)\left[1 - \frac{r^*(T)}{r}\right]. \tag{6}$$

Note that this expression is employed only in the range of cluster sizes $r^*(T_{d1}) \leqslant r \leqslant r^*(T_{d2})$, i.e., at a sufficiently large distance from $r^*(T_n)$.

Taking into account that

$$r^*(T) = 2\sigma/\Delta G(T), \tag{7}$$

where $\sigma$ is the critical nucleus–liquid surface free energy, and $\Delta G$ is the difference between the free energies of the liquid and crystal per unit volume of crystal, and assuming that $\sigma$ depends only weakly on the temperature, one may rewrite Eq. (5) as

$$\sigma = \frac{1}{2}\Delta t_0 U(T_n,\infty)\Bigg/\left[\frac{1}{\Delta G(T_{d2})} - \frac{1}{\Delta G(T_{d1})} + \frac{1}{\Delta G(T_n)}\ln\left[\frac{\frac{1}{\Delta G(T_{d2})} - \frac{1}{\Delta G(T_n)}}{\frac{1}{\Delta G(T_{d1})} - \frac{1}{\Delta G(T_n)}}\right]\right]. \quad (8)$$

Hence, it is possible to calculate the average value of $\sigma$ in the temperature range $T_n$–$T_{d2}$ from the experimental values of $\Delta t_0$, $U(T_n,\infty)$ and $\Delta G$. It should be emphasized that in doing so neither *nucleation rate* nor *time lag* for nucleation are required.

## 3. Materials and methods

The dissolution of sub-critical nuclei at several development temperatures was investigated in two glasses having compositions close to $Li_2O \cdot 2SiO_2$ and $Na_2O \cdot 2CaO \cdot 3SiO_2$. Analytical grade carbonates of lithium, sodium, and calcium, and amorphous silicon dioxide were used for their synthesis in a platinum crucible at ~1500°C in an electric furnace. The analyzed compositions of glass samples are listed in Table 1.

To determine the number density of the nucleated crystals we employed the Tammann method using different development temperatures. The heat-treatments were performed in a vertical electric furnace that was capable of maintaining the temperatures to ±1°C. We measured the number of crystals and their sizes with Jenaval and Neophot optical microscopes.

To calculate the number of developed crystals the standard Eqs. (9) and (10), derived for cubic particles [20] and for prolate ellipsoids [21], respectively, were employed:

$$N = \frac{N_S}{3b}, \quad (9)$$

Table 1
Chemical compositions of the glass samples in mol% by analysis

| Glass | $SiO_2$ | $Li_2O$ | $Na_2O$ | CaO |
|---|---|---|---|---|
| L2S | 67.1 | 32.9 | – | – |
| N2C3S | 49.9 | – | 17.1 | 33.0 |

$$N = \frac{N_S}{d_{min}K(q)}, \quad K(q) = \frac{1}{2}\left[\frac{1}{q} + \frac{q\ln\left(\frac{1+\sqrt{1-q^2}}{q}\right)}{\sqrt{1-q^2}}\right],$$

$$q = d_{min}/d_{max}, \quad (10)$$

where $N_S$ is the number density of crystal traces on the sample's cross-sections (polished surfaces), $2b$ is the length of a cube edge and $d_{max}$ and $d_{min}$ are the ellipsoid's diameters.

## 4. Experimental results

The $Na_2O \cdot 2CaO \cdot 3SiO_2$ (N2C3S) crystals have a cubic morphology at all temperatures under study. The $Li_2O \cdot 2SiO_2$ (L2S) crystals, grown at the development temperatures, are prolate ellipsoids, with diameter ratio $d_{max}/d_{min} = 1.4$ to 1.6. The crystals grown at the nucleation temperatures $T_n \leqslant T_g$ have an extended form, which we approximated as right-angled parallelepipeds with square basis, having a ratio of height to side of the basis $\beta = 2h/2a \cong 2.60$.

The kinetic curves $N(T_n,t)$, obtained for different development temperatures ($T_{d1}, T_{d2} > T_{d1}$) and fixed $T_n$, are shown in (Figs. 1 and 2). Figs. 3 and 4 show the sizes of the largest crystals as a function of heat-treatment time at the nucleation temperatures.

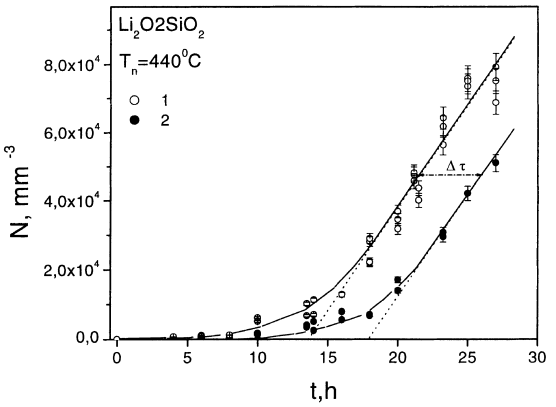


Fig. 1. Number density of $Li_2O \cdot 2SiO_2$ crystals developed at $T_{d1} = 530$°C (1) and $T_{d2} = 640$°C (2) as a function of nucleation time at $T_n = 440$°C.

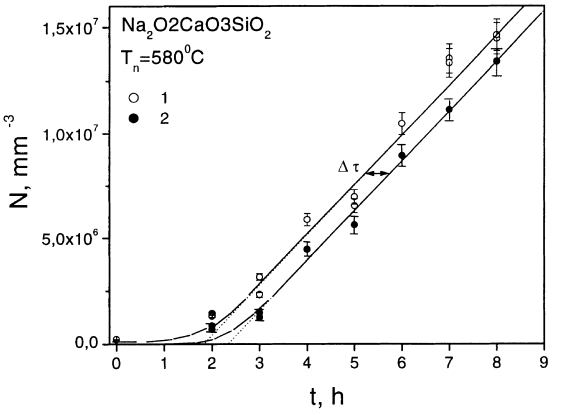


Fig. 2. Number density of $Na_2O \cdot 2CaO \cdot 3SiO_2$ crystals developed at $T_{d1} = 650°C$ (1) and $T_{d2} = 720°C$ (2) as a function of nucleation time at $T_n = 580°C$.

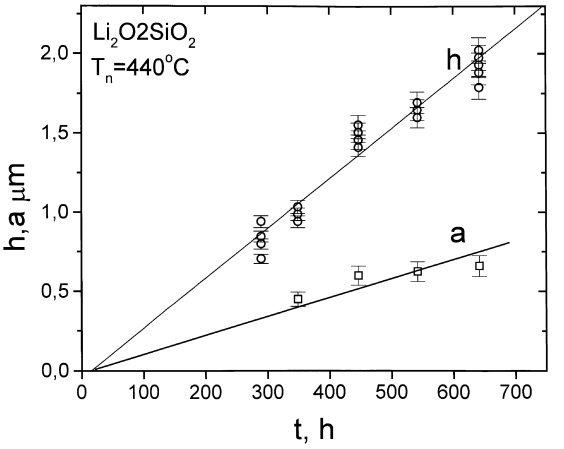


Fig. 3. Sizes $h$ and $a$ of the largest $Li_2O \cdot 2SiO_2$ crystals vs time of heat treatment at $T_n = 440°C$.

As expected, the kinetic curves obtained by the development method shift in the direction of increasing time when $T_d$ is increased (Figs. 1 and 2). The shift is more pronounced in the case of L2S glass. In the case of N2C3S glass, despite the fact that the difference in N is within the experimental errors, the $N(T_n, r^*(T_{d1}), t)$ data are systematically higher than the $N(T_n, r^*(T_{d2}), t)$ data. The number of crystals nucleated at $T_{d1}, N(T_n, t = 0)$ is negligible compared to the difference between curves $N(T_n, r^*(T_{d1}), t)$ and $N(T_n, r^*(T_{d2}), t)$.

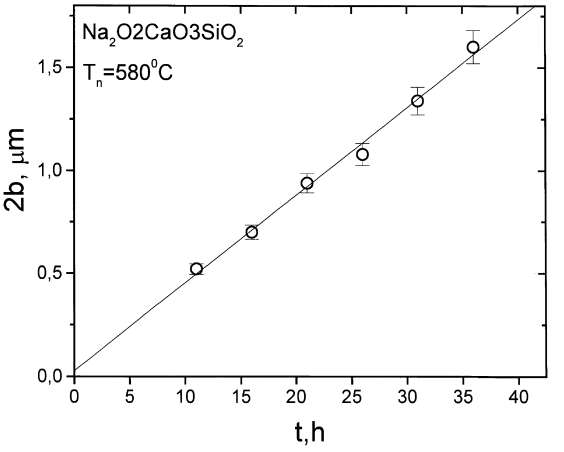


Fig. 4. Size (the length of a cube edge) of the largest $Na_2O \cdot 2CaO \cdot 3SiO_2$ crystals vs time of heat treatment at $T_n = 580°C$.

Figs. 5–7 show literature data that also demonstrate a decrease of the number of developed crystals with increasing $T_d$. According to Eq. (5), the shift of the $N(t)$ plots is strongly affected by $U(T_n)$, and varies proportionally to $1/U(T_n)$. Indeed, the dependence $\Delta t_0(T_n, r^*(T_{d1}), r^*(T_{d2}))$ on $1/U(T_n)$ at practically fixed development temperatures (see Table 2) is close to the expected one (Fig. 8). The inequality $N(T_d = 560°C) > N(T_d = 600°C)$ at $T_n = 476°C$ was also reported in [22]

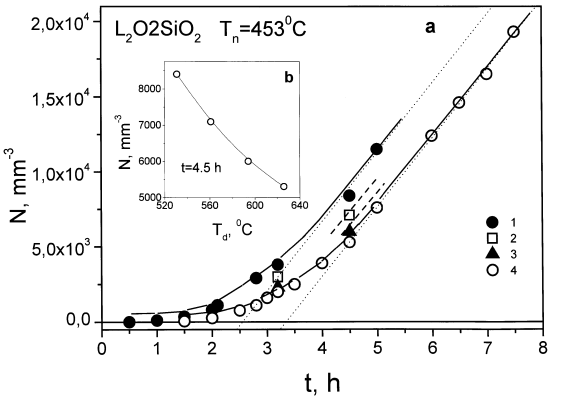


Fig. 5. (a) Number density of $Li_2O \cdot 2SiO_2$ crystals developed at $T_d = 530°C$ (1), 560°C (2), 594°C (3) and 626°C (4) as a function of nucleation time at $T_n = 453°C$. (b) Number density of $Li_2O \cdot 2SiO_2$ crystals nucleated at $T_n = 453°C$ for 4.5 h vs development temperature [7].

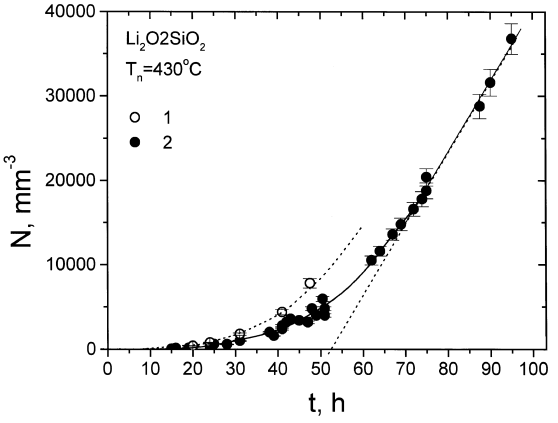


Fig. 6. Number density of $Li_2O \cdot 2SiO_2$ crystals developed at $T_{d1} = 530°C$ (1) and $T_{d2} = 626°C$ (2) as a function of nucleation time at $T_n = 430°C$ [23].

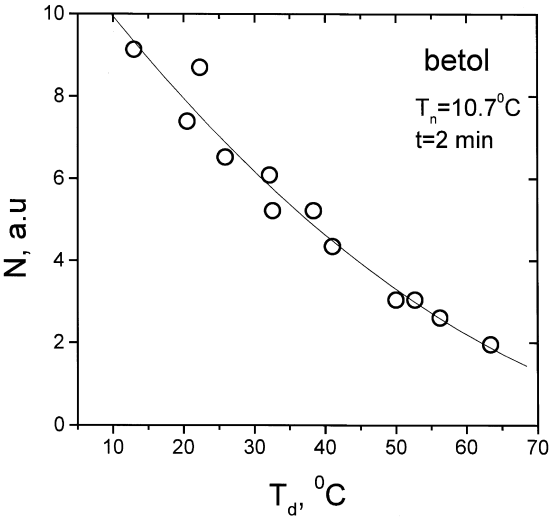


Fig. 7. Number of betol crystals nucleated at $T_n = 10.7°C$ for 2 min vs development temperature [6].

for L2S glass. However, owing to the high nucleation temperature and correspondingly high crystal growth velocity $U(T_n)$, the effect was very weak.

## 5. Determination of the surface energy: a first attempt

Eq. (8) is used here to estimate the critical nucleus–liquid interfacial energy. However, this

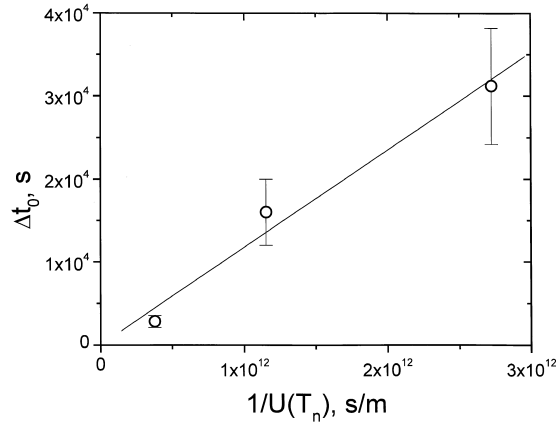


Fig. 8. $\Delta t_0$ vs $1/U(T_n)$ for $Li_2O \cdot 2SiO_2$ crystals.

equation has been derived under the assumption that the clusters of the new phase are spherical. In order to apply the theory to the interpretation of the experimental data, we have to redefine the respective quantities via the introduction of an effective cluster radius and effective surface energy for the equivalent spherical nuclei. To solve this task we assumed that the crystal shape is size independent. Hence the critical crystals of L2S are parallelepiped shaped, with $\beta = 2h/2a \cong 2.60$. The critical N2C3S crystals are cube shaped, with edge $2b$. It can be shown that the critical sizes of a parallelepiped and a cube are

$$\begin{aligned} h^* &= 2\sigma_a/\Delta G, \ldots \\ a^* &= 2\sigma_h/\Delta G, \ldots \text{(parallelepiped)}, \end{aligned} \tag{11a}$$

$$b^* = 2\sigma_b/\Delta G, \quad \text{(cube)} \tag{11b}$$

Here $\sigma_a, \sigma_h$, are the surface energy of the base and side facets of the parallelepipeds, respectively, and $\sigma_b$ is the facet surface energy of a cube. Hence, the work of formation of critical nuclei having parallelepiped or cubic shape are, respectively:

$$W_p^* = 32\sigma_h^2\sigma_a/\Delta G^2, \tag{12a}$$

$$W_{cu}^* = 32\sigma_b^3/\Delta G^2. \tag{12b}$$

We now introduce the effective surface energy of spherical nuclei, $\sigma_{sph}$, using the conditions:

Table 2
Experimental conditions and surface energy for several glasses[a]

| Glass | $T_n$ (°C) | $U(T_n,\infty)$ (m/s) | $\beta = U_h/U_a$ | $T_{d1}$ (°C) | $T_{d2}$ (°C) | $\Delta t_0$ (s) | $\sigma_h$ (J/m$^2$) | $\sigma_a$ (J/m$^2$) | $\sigma_b$ (J/m$^2$) | $\sigma_{sph}$ (J/m$^2$) |
|---|---|---|---|---|---|---|---|---|---|---|
| L2S | 440 | $U_h$ $8.67\times10^{-13}$ | 2.60 | 530 | 640 | 16020 | 0.82 | 2.13 | – | 1.40 |
| N2C3S | 580 | $U_b$ $5.92\times10^{-12}$ | – | 650 | 720 | 1740 | – | – | 1.2 | 1.49 |
| L2S [23] | 430 | $U_h$ $3.67\times10^{-13}$ | 2.66 | 530 | 626 | 31200 | 0.80 | 2.12 | – | 1.37 |
| L2S [7] | 453 | $U_h$ $26.5\times10^{-13}$ | 2.66 | 530 | 626 | 2847 | 0.64 | 1.71 | – | 1.11 |

[a] The following values of $\Delta G$ were used for calculations:
*L2S glass:* $\Delta G$ (J/m$^3$) $= 8.431\times10^8 - 548258.656T - 73.002T^2$ T(K) , which fits well the experimental data [24] in the temperature range under study.
*N2C3S glass:*

$$\Delta G = -\frac{\Delta H_m}{T_m}(T_m - T) - \int_T^{T_m} \Delta C_p\,dT' + T\int_T^{T_m} \frac{\Delta C_p}{T'}\,dT',$$

where $\Delta H_m$ and $T_m$ are the latent heats of melting per mole and melting point, respectively. $\Delta C_p = C_p^C - C_p^L$ is difference in specific heats between the crystalline and liquid phases. $\Delta H_m = 87\,900$ J/mol [25], $\Delta C_p$[J/mol K] $= 71.41 - 103.3\times10^{-3}T - 56.97\times10^5/T^2$ [26].

$$W_p^* = W_{sph}^* = \frac{16\pi}{3}\frac{\sigma_{sph}^3}{\Delta G^2} \quad \text{or} \quad W_{cu}^* = W_{sph}^*. \tag{13}$$

The following equations can then be derived for $\sigma_{sph}$ from Eqs. (12a), (12b) and (13):

$$\sigma_{sph} = \left[\frac{6}{\pi}\sigma_h^2\sigma_a\right]^{1/3} \quad \text{or} \quad \sigma_{sph} = \left[\frac{6}{\pi}\sigma_b^3\right]^{1/3}. \tag{14}$$

Thus, the nucleation rate of the spherical nuclei with $\sigma_{sph}$ is close to those of nuclei having parallelepiped or cubic shape, with surface energies $\sigma_h$ and $\sigma_a$ or $\sigma_b$, respectively.

We used the experimental values of $\Delta t_0$ and $U(T_n,\infty)$ and literature data for $\Delta G$ to estimate the surface energy from Eq. (8). Table 2 presents the results of these calculations for glasses L2S ($T_n = 440$°C) and N2C3S ($T_n = 580$°C), and also a result using literature data for the glass L2S ($T_n = 453$°C and 430°C).

For the sake of comparison we collected different data on the surface energy of both liquid–air, $\sigma_{l/g}$, and of liquid–crystal interfaces for glass compositions close to those under study. Table 3 includes the experimental values of $\sigma_{l/g}$ as well as the values calculated by Appen's equation [27]. It is obvious that the nucleus/liquid surface energy cannot be larger than that of the liquid-gas interface, however, according to Tables 2 and 3, $\sigma_{sph} > \sigma_{l/g}$ (hereinafter, for comparison purposes, we will focus on $\sigma_{sph}$). It should be recalled that $\sigma_{l/g}$ relates to a planar interface while $\sigma_{sph}$ relates to a spherical nucleus. However, a consideration of the size effect on the value of $\sigma$ could only strengthen this inequality.

Table 3 also shows the crystal–liquid surface energy calculated from nucleation data by different methods ($\sigma^*, \sigma^{**}$) as well as $\sigma_T$ from Eq. (1). All these values are much smaller than $\sigma_{sph}$ of Table 2. When $\sigma_{sph}$ together with the thermodynamic driving force $\Delta G$ (for bulk phase crystallization) is used, the nucleation rate calculated by CNT is vanishingly small. However, nucleation indeed occurs and is experimentally observed. Consequently, we have to search for some hidden drawback in the estimation of $\sigma_{sph}$. In order to do so, we have to make a brief excursion into the thermodynamics underlying CNT.

Table 3
Liquid–gas and liquid–crystal surface energies calculated from nucleation data

| Glass composition (mol%) | $\sigma_{l/g}$, calcul. [27] ($J/m^2$) | $\sigma_{l/g}$, exper. ($J/m^2$) | $\sigma^*$ [15] ($J/m^2$)[a] | $\sigma^{**}$ ($J/m^2$)[b] | $\sigma_T$ for $\alpha = 0.45$ ($J/m^2$) |
|---|---|---|---|---|---|
| 33.3 $Li_2O$–66.7 $SiO_2$ | 0.343 | 0.320 [28] | 0.202 | 0.152–0.156, $450°C < T < 485°$ C [15] | 0.197 |
| 16. 91 $Na_2O$ 33.41 CaO 49.68 $SiO_2$ | 0.363 | – | 0.185 | 0.099–0.110, $580°C < T < 685°C$ [30] | 0.186 |
| 17. 9 $Na_2O$ 35.0 CaO 57. 1 $SiO_2$ | 0.346 | 0.338 [29] | – | – | – |

[a] $\sigma^*$ calculated from the slope of $\ln(I_{st} \cdot t_{ind} \cdot \Delta G^2)$ vs $1/T\Delta G^2$ plots, where $t_{ind}$ is the induction time of nucleation on the assumption that $\sigma^*$ does not change with $T$.
[b] $\sigma^{**}$ calculated from fit of nucleation rate to CNT, using the theoretical value of the pre-exponential term, thus allowing $\sigma^*$ to vary with $T$.

## 6. A side-step into the thermodynamics of CNT

The determination of the work of critical cluster formation employed in CNT is based on the thermodynamic description of heterogeneous systems developed by Gibbs [8]. According to that author, a real inhomogeneous system – in our case a crystalline cluster in its melt – is replaced by an idealized model system consisting of two homogeneous phases divided by a mathematical surface of zero thickness (see Fig. 9). The thermodynamic potential of the system is expressed then as the sum of the bulk contributions of cluster and ambient phase, and a correction term. The latter is essentially (but not exclusively) given by the product $\sigma \cdot A$, where $A$ is the surface area.

The value of the correction term and, consequently, the value of $\sigma$, depends on the choice of the reference states for the description of the bulk properties in the idealized model system. Following Gibbs, the properties of the respective macrophases are chosen as such reference states, which may coexist in thermal equilibrium at planar interfaces under the given thermodynamic conditions. This choice of the reference state is quite appropriate for large critical clusters, since it reflects, in this limit, the real physical situation. As a consequence, $\sigma$ corresponds with good accuracy to its value for a planar interface, i.e., the capillarity approximation holds.

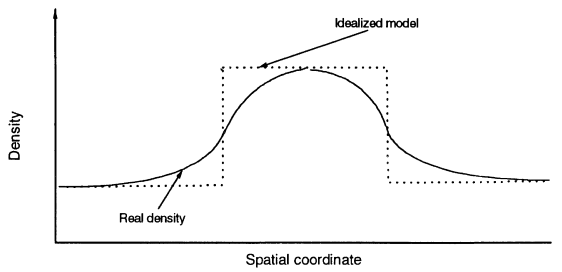


Fig. 9. Schematic density profile of a crystalline cluster.

For small critical clusters, however, the properties of the macroscopic reference state may deviate significantly from the actual bulk properties of the cluster. Nevertheless, as shown by Gibbs, one may retain the macroscopic properties as reference states for the thermodynamic description. However, in order to arrive at the correct results for the thermodynamic potential, in general, and at the work of critical cluster formation, in particular, size dependent corrections for the value of the surface tension have to be introduced (e.g., [31]).

As shown recently for segregation processes for both solid and liquid solutions [31,32], it is possible to generalize Gibbs' approach by choosing reference states for the bulk properties of the cluster that correspond to the real physical situation, independent of cluster size. The equation for the work of critical cluster formation retains the same form as in the standard of approach of Gibbs. However, the values of $\sigma$ and $\Delta G$ for the cluster, in general, differ from those of the respective macrophases. These alternatively defined values of $\Delta G$ – and *not* the value of $\Delta G$ according to Gibbs' choice of the reference state are the real driving force for critical cluster formation and

further growth of the clusters. The growth of the clusters is driven not by the value of $\Delta G$ between two reference states, but by the respective differences in the real physical states.

We thus come to the following conclusion: The standard approach of Gibbs is correct for the description of thermodynamic properties of heterogeneous systems down to very small cluster sizes. Deviations of the properties of the reference states from the state of real system can be compensated by appropriately introduced curvature corrections to the surface tension. However, in order to model the kinetics of cluster growth, one has to know the value of $\Delta G$ for the real states of the cluster in the ambient phase. These values of $\Delta G$ may be quite different from the respective quantities employed in Gibbs' thermodynamic approach.

The difference between the values of $\Delta G$ for the reference states, employed in Gibbs' thermodynamic description, and the driving force of cluster growth, which is determined by the real physical state of the cluster, is the basic origin of the problems in the determination of $\sigma$ discussed above. These arguments will be employed in the next section to resolve this discrepancy.

## 7. Determination of the surface energy: final solution

Taking into account the analysis given in the previous section, let us now consider in more detail the possible reasons for the origin of the discrepancy between the values of the surface energy, $\sigma_{\mathrm{sph}}$, calculated from dissolution effects and $\sigma^{**}$ calculated from the fit of nucleation rate data. Remember that both methods refer to nuclei of near critical sizes, thus only a reference to size effects does not resolve the problem.

However, not only the surface energy but also the thermodynamic driving force of the transformation may be size dependent. Whereas the problem of the size dependence of the surface tension has been the subject of intensive analysis, e.g., [16,17,33], the situation with respect to $\Delta G$ still remains obscure. As outlined in the previous section, such analysis may not even be required if one remains within the classical thermodynamic approach of Gibbs.

Let us now estimate the driving force for two models of critical cluster formation. First we consider the situation that the critical cluster and the newly evolving phase have the same composition as the melt. Using the classical approach, the chemical potential per ambient phase particle in the newly evolving phase (specified by $\alpha$) is

$$\begin{aligned} &\mathrm{d}\mu_\alpha = \upsilon_\alpha \,\mathrm{d}p_\alpha, \\ &\mu_\alpha(p_\alpha) = \mu_\alpha(p) + \upsilon_\alpha(p_\alpha - p). \end{aligned} \tag{15}$$

If $p_\alpha$ refers to the pressure in a cluster of critical size, we obtain $\mu_\alpha(p_\alpha) = \mu_\beta(p)$ ($\beta$ specifies the parameters of the ambient melt)

$$p_\alpha - p = \frac{1}{\upsilon_\alpha}(\mu_\beta(p) - \mu_\alpha(p)) = \frac{\Delta\mu}{\upsilon_\alpha} = \Delta G_\infty. \tag{16}$$

In these derivations, $\upsilon_\alpha$ is considered as a constant equal to the respective value in the evolving macrophase.

It is reasonable to assume that the critical nucleus is less ordered than the corresponding bulk phase. Thus, proceeding in the same way as above, $\upsilon_\alpha$ must be replaced by a higher value $\langle\upsilon_\alpha\rangle$ corresponding to some average of this quality in the considered range of pressure. Thus, we get

$$p_\alpha - p = \Delta\mu/\langle\upsilon_\alpha\rangle = \Delta G, \quad \Delta G < \Delta G_\infty. \tag{17}$$

We thus may write

$$\Delta G = K(r)\Delta G_\infty, \quad K(r) < 1, \tag{18}$$

where $r$ is the size of the critical crystal.

Another reason that could lead to the reduction of the thermodynamic driving force for cluster growth consists in the following. According to a recent model [34,35], glass-forming melts can be considered as solutions of oxide components and salt-like products. (Here we should emphasize that the concentrations of any species of melt, in general, are less than 1. Thus, the concept of stoichiometric melt as the melt consisting only of structural units of the melt composition looses justification.) Critical cluster formation should then be considered as a segregation process in a multi-component solution. As shown in detail for a model system in [32], the driving force may be

(and in general is) much smaller than the macroscopic value. This effect is due to deviations of the composition of the critical cluster from the respective values for the evolving macrophase. Therefore, Eq. (18) is well founded. Further on we will derive conclusions from this relationship.

## 8. Driving force and specific surface energy for critical and near-critical cluster sizes.

The methods to calculate $\sigma$ based on the dissolution of sub-critical nuclei (the present method) or on the fit of nucleation data to CNT do not provide the surface energy directly, but instead, only its combinations with the thermodynamic driving force. In particular, $\sigma_{\mathrm{sph}}$ is calculated from measured $\Delta t_0$ (see Eq. (5))

$$\Delta t_0 = 2\sigma_{\mathrm{sph}} f(1/\Delta G)/U \tag{19}$$

and $\sigma^{**}$ – from the thermodynamic barrier for nucleation

$$W^* \sim {\sigma^{**}}^3/\Delta G^2. \tag{20}$$

It should be noted that in the latter case the effect of the surface energy in the pre-exponential term of the nucleation rate equation is neglected (this effect is small).

The comparison between $\sigma^{**}$ and $\sigma_{\mathrm{sph}}$ allows us to estimate the coefficient $K(r)$ in Eq. (18). Let us denote the true value of surface energy corresponding to the real state of the cluster by $\sigma$ (i.e., the value of the specific surface energy if Eq. (18) is taken into account in its estimation). Then, employing Eqs. (19) and (20) and taking into account that $U \sim \Delta G$, one may write the following equations connecting $\sigma$ with $\sigma_{\mathrm{sph}}$ and $\sigma^{**}$

$$\sigma = K(r)^2 \sigma_{\mathrm{sph}}, \tag{21}$$

$$\sigma = K(r)^{2/3} \sigma^{**}. \tag{22}$$

The combination of Eqs. (21) and (22) yields

$$K = (\sigma^{**}/\sigma_{\mathrm{sph}})^{3/4}. \tag{23}$$

Thus, both methods provide the same values of $\sigma$ when the reduced thermodynamic driving force, $K(r)\Delta G_\infty$, is used.

Using the data of Tables 2 and 3, we have $0.19 < K < 0.23$ and $K = 0.13$, for L2S and N2C3S glasses, respectively. A substitution of $K$ into Eq. (21) or (22) gives $50 < \sigma < 60$ mJ/m$^2$ and 26 mJ/m$^2$ for L2S and N2C3S glasses, respectively. It should be emphasized that these values are less than $\sigma_{\mathrm{l/g}}$ as we expected (see Table 3).

It is possible that the discussed reason for the difference between $\sigma_{\mathrm{sph}}$ and $\sigma^{**}$ is not unique. Nevertheless our estimation of $K$ shows that $\Delta G$ can differ significantly from $\Delta G_\infty$ and calls attention to the correct use of the thermodynamic driving force for a proper treatment of crystal nucleation kinetics in liquids. This conclusion is consistent with a new approach to determination of the work of critical cluster formation [32]. According to that approach, 'both the structure and composition of the critical clusters may deviate significantly from the respective properties of the evolving macrophases'.

## 9. Conclusion

We provided new experimental evidence for the dissolution of nuclei that are converted into sub-critical sizes by a temperature increase. Based on this phenomenon, we proposed a new method to determine the nucleus/liquid surface energy and applied it to two stoichiometric glasses.

The values of the nucleus/liquid surface energy determined by this method, employing macroscopic values for the thermodynamic driving force of crystallization, are much larger than those obtained from a fit of nucleation rate data to CNT. It is shown that this discrepancy may be eliminated if a reduction of thermodynamic driving force for crystallization of near-critical size clusters is allowed for. The possible reasons for such reduction are discussed in detail.

## References

[1] G. Tammann, Z. Phys. Chem. 25 (1898) 441.
[2] M. Ito, T. Sakaino, T. Moriya, Bull. Tokyo Inst. Technol. 88 (1968) 127.
[3] V.N. Filipovich, A.M. Kalinina, Neorgan. Mater. 4 (1968) 1532.

[4] J.W. Christian, The Theory of Transformation in Metals and Alloys, Part I, Pergamon, Oxford, 1981, p. 584.
[5] M. Volmer, A. Weber, Z. Phys. Chem. 119 (1926) 277.
[6] G.L. Mikhnevich, I.F. Browko, Phys. Sowjetunion 13 (1938) 113.
[7] A.M. Kalinina, V.M. Fokin, V.N. Filipovich, Fiz. Khim. Stecla 2 (1976) 294.
[8] J.W. Gibbs, The Collected Works, Vol. 2, New York, 1928.
[9] I. Gutzow, J. Schmelzer, The Vitreous State, Springer, Berlin, 1995, p. 469.
[10] K.F. Kelton, Solid State Phys. 45 (1991) 75.
[11] E.D. Zanotto, J. Non-Cryst. Solids 89 (1987) 361.
[12] E.G. Rowlands, P.F. James, Phys. Chem. Glasses 20 (1979) 1, 9.
[13] E.D. Zanotto, P.F. James, J. Non-Cryst. Solids 74 (1985) 373.
[14] V.M. Fokin, A.M. Kalinina, V.N. Filipovich, J. Cryst. Growth 52 (1980) 115.
[15] P.F. James, J. Non-Cryst. Solids 73 (1985) 517.
[16] M.C. Weinberg, E.D. Zanotto, S. Manrich, Phys. Chem. Glasses 33 (1992) 99.
[17] V.M. Fokin, E.D. Zanotto, J. Non-Cryst. Solids 265 (2000) 105.
[18] J. Deubener, M.C. Weinberg, J. Non-Cryst. Solids 231 (1998) 143.
[19] V.N. Filipovich, T.A. Jukovskaiy, Fiz. Khim. Stekla 14 (1988) 300.
[20] S.A. Saltikov, Stereometric Metallography, Metallurgia, Moscow, 1970, p. 376.
[21] R.T. DeHoff, F.N. Rhines, Trans. Metall. Soc. AIME 221 (1961) 975.
[22] P.F. James, Phys. Chem. Glasses 15 (1974) 95.
[23] V.M. Fokin, PhD thesis, Institute of Silicate Chemistry of Russian Academy Sciences, 1980.
[24] K. Takahashi, T. Yoshio, J. Ceram. Soc. Japan 81 (1973) 524.
[25] P.F. James, Phys. Chem. Glasses 15 (1974) 95.
[26] V.I. Babushkin, G.M. Matveyev, O.P. Mchedlov-Petrossyan, Thermodynamics of Silicates, Springer, Berlin, 1985.
[27] J.M.F. Navaro, El Vidrio, CSIC, Spain, 1991.
[28] L. Shartsis, S. Spinner, J. Res. Nat. Bur. Stand. 46 (1951) 385.
[29] A.A. Appen, K.A. Schishov, S.S. Kaylova, Silicattechnik 4 (1953) 104.
[30] O.V. Potapov, V.M. Fokin, V.N. Filipovich, J. Non-Cryst. Solids 247 (1999) 74.
[31] I.W.P. Schmelzer, Curvature dependent surface tension and nucleation theory, in: Nucleation Theory and Aplications, Joint Institute for Nuclear Research Publishing House, Dubna, Russia, 1999, p. 268.
[32] J.W.P. Schmelzer, J. Schmelzer Jr., I.S. Gutzow, J. Chem. Phys. 112 (2000) 3820.
[33] J.W.P. Schmelzer, I. Gutzow, J. Schmelzer Jr., J. Colloid Interface Sci. 178 (1996) 657.
[34] B.A. Shakhmatkin, N.M. Vedisheva, M.M. Shultz, A.C. Wright, J. Non-Cryst. Solids 177 (1994) 249.
[35] B.A. Shakhmatkin, N.M. Vedisheva, J. Non-Cryst. Solids 171 (1994) 1.